

Polymer/clay Nanocomposite: A Viable Anti-Corrosion Coating for Geothermal Applications

Jennifer Espartero-Dales¹, Al Christopher de Leon², Eugene Caldona³ and Rigoberto Advincula⁴

¹Energy Development Corporation, Southern Negros Geothermal Production Field, Ticala, Valencia, Philippines

^{2,4} Department of Macromolecular Science and Engineering, Case Western Reserve University, Cleveland, Ohio, USA

³University of the Philippines- Diliman, Quezon City, Metro Manila, Philippines

espartero.jc@energy.com.ph

Keywords: nanocomposite coating, high temperature, corrosion, electrochemical testing

ABSTRACT

Polymer modification has been attracting the attention of the scientific community due to its process of combining attractive properties of different materials and fusing it into a hybrid high performance material. These properties depend on the type of environment and its application. Due to the harsh conditions imposed by geothermal fluids to ordinary materials of construction, high performance materials are desired to lessen the frequency or even eliminate maintenance cleaning of surface components and to prolong the service life of pipelines and other surface equipment that are critically affected by erosion-corrosion phenomenon. To further enhance the mechanical properties of a high performance polymer material, nanofillers are usually incorporated in the polymer matrix to make up a nanocomposite. In this study, a nanocomposite (PCN-R-oMMT) made of toughened polymer and organically modified montmorillonite was synthesized to be used as a coating. The enhancement of the mechanical properties of the polymer by addition of oMMT by its intercalation/exfoliation into the polymer matrix was determined using X-Ray Diffraction (XRD), thermogravimetric tests (TGA & DSC), hardness test, and adhesion test. To determine the viability of the synthesized coating in corrosive environment, it was applied to a carbon steel coupon and immersed in simulated acidic geothermal brine. Electrochemical impedance spectroscopy (EIS) and potentiodynamic polarization scans (PPS) were conducted to assess the protection efficiency of the coating. The stability and the protection efficiency of the PCN-R-oMMT were also evaluated under high temperature and high pressure conditions.

1. INTRODUCTION

Geothermal production is hindered by scaling and corrosion problems. Both of these problems entail high cost and pose high risk in terms of material and environmental safety. The chemistry of each production well is unique, making it challenging to find an anti-corrosion solution that would fit into the nature of the fluid. This is especially true of acid-producing wells that corrode metal casing and pipelines at a very fast rate. Most of these wells are unusable due to the aggressive behavior of their fluids because of fast metal dissolution destroying the integrity of the pipe. The utilization of these wells, therefore, is dependent on the use of an effective corrosion prevention technology that would significantly lower the rate or retard the corrosion process.

One way of retarding the effects of corrosion is by application of coatings. Due to the relatively high temperature nature of a geothermal process, coatings to be applied must have good thermal stability and high resistance to chemical attack. The issue of hardness and adhesion also needs to be considered in choosing the right material since geothermal fluid does not only contain corrosive agents but may contain high amounts of suspended solids. These high velocity solids will impinge on the walls of the pipe, eroding the metal. Erosion together with corrosion would have a synergistic effect on the rate of metal dissolution, making it a critical factor to consider in operating a highly erosive and corrosive environment.

Polymer modification has been attracting the attention of scientific community due to its process of combining attractive properties of different materials and fusing it into a hybrid high performance material. These properties depend on the type of environment and its application. For this study, we have chosen to modify a polymer (PCN) to tailor the needs of a typical acidic geothermal well. The polymer has excellent properties that fit the requirements such as near-zero shrinkage upon polymerization, low surface free energy, low water absorption, good thermal stability, and good mechanical properties, as observed in the studies of Ishida et al. (2011). Zhou et al. (2013) reported that although there has been few studies conducted regarding the use of PBZ for anticorrosion, polybenzoxazines have the potential for application as corrosion protective coating due to their unique properties, such as low water absorption, low surface free energy, near-zero shrinkage, and excellent dielectric properties, which are superior to those of epoxy resins and conventional phenolics. However, the polymer is brittle and needs to be modified to be able to expand the limits of its application as discussed by Ishida and Allen (1996). Several approaches have been designed to toughen thermosetting materials and one of the most promising is the modification with rubber. It has been found that rubber modification is an effective approach to overcome the inherent brittleness of thermosets. For instance, physical blends of polymer and rubber have improved fracture toughness without undue sacrifices to the desirable properties, as shown by the study of Jang and Yang (2000). Hence, in our study, the polymer is toughened by blending the synthesized polymer with rubber.

To further enhance the mechanical properties of a high performance polymer material, nanofillers are usually incorporated in the polymer matrix to make up a nanocomposite. One critical factor in making an effective polymer nanocomposite is the type of nanofiller to be used. Based on the study conducted by Hung et al. (2011), clay nanocomposites show enhanced physical properties even with a small amount of added clay because the nanoscale dimensions of the clay particles yield a large contact area between the polymer matrix and the filler. The structure of clays also imparts an excellent barrier that provides low gas permeability and

enhanced anticorrosive properties. The dispersion of clay was found to boost the thermal stability, as reported by Lan et al. (1994). Enhancement of the mechanical properties was reported by Tyan et al. (1999) while the molecular barrier was reported by Wang et al. (2001) and Lan et al. (1994). One critical factor is the type of nanofiller to be used. Clays are found to be one of the ideal nano reinforcements for polymers, because of its high intercalation chemistry, high aspect ratio, ease of availability and low cost, based on the study of Azeez et al. (2012) on epoxy clay nanocomposites. It was shown in the study of Arthur et al. (2011) that the use of montmorillonite (MMT) has enhanced the mechanical properties of the polymer at very low loading (<5 wt%). Montmorillonite is an example of a smectite clay with a 2:1 structure, which allows sharing of oxygen between Al and Si. It is known to have a good high-aspect ratio, high surface area, and environment friendly. However, it is hydrophilic in its natural state which makes it difficult to be dispersed in most polymers and could easily aggregate. In order for it to be used as a nanofiller, its layered silicates should be organically modified first. This is usually done by exchanging the cations present at the silicate surfaces of MMT with long chain alkyl ammonium cation, making it organophilic which will be now compatible with most polymers.

The objective of this study is to synthesize a polymer/clay nanocomposite (PCN-R-oMMT) coating that is designed for application in an acidic geothermal well pipeline, and test its corrosion protection efficiency and mechanical stability under harsh geothermal conditions.

2. METHODOLOGY AND INSTRUMENTATION

The FT-IR spectroscopy was done with FTIR Spectrometer and scanned between 4000 and 400 cm^{-1} . All spectra were recorded with nominal spectral resolution of 2 cm^{-1} , and 128 scans were collected and averaged for each spectrum.

Adhesion test measurement was performed according to the ASTM standard test method D-3359 for measuring the adhesion strength by tape test. A blade handle equipped with a four-tooth 2.4-mm spacing coarse blade was used to make the cross-cut configuration through the coatings. The coating was brushed lightly with a soft brush after each cut to remove any debris, detached flakes, or ribbons of coatings from the surface. Scotch tape 51596 was placed on the cut surface and rubbed with the eraser on the end of a pencil to ensure good contact with the film and then removed rapidly after 90s. The grid areas were inspected for possible removal of the coating from the substrate, and adhesion strength was rated in accordance with the scale provided by the ASTM.

Hardness test measurement was performed using a pencil hardness tester which meets the ASTM standard D 3363. For this test, pencils of increasing hardness values are moved over the surface in a precisely defined way until one damages the surface. Sufficient pressure must be applied to either cut or damage the coating or to crush the lead pencil point. Repeat the test as many times as possible until a definite observation is made. If scratching or damage of the surface occurs, proceed with the next softer pencil grade and repeat the testing process until a pencil lead grade is found which crushes and does not damage the coating. If crushing of the hardest lead should occur, the coating is therefore extremely hard and beyond the measuring range of this test.

Electrochemical measurements for the evaluation of anti-corrosion property were done using a Potentiostat, with platinum as the counter electrode, Ag/Ag⁺ in 0.5 M NaCl as the reference electrode, and the carbon steel substrates as the working electrodes. Potentiodynamic polarization scan (PPS) was performed by scanning from -0.025 to +0.025 V vs Ag/Ag⁺ reference electrode (0.5 M NaCl) about the open circuit potential (OCP) while electrochemical impedance spectroscopy (EIS) was performed for seven frequency decades from 10 mHz to 100 kHz, with an amplitude of 10 mV with respect to the OCP.

3. RESULTS AND DISCUSSION

3.1 X-Ray Diffraction (XRD)

One of the critical processes in ensuring optimal properties of PCN is the modification of the cations at the silicates interlayer spacing by cationic exchanged with long-chain alkyl ammonium cation. XRD was conducted to determine the swelling of the nanoclay by calculating the d-spacing of the natural MMT and the organically modified MMT(oMMT). Figure 1a shows the XRD spectra of MMT and oMMT. By using the spectra result and Bragg's law, d-spacing of MMT and oMMT are calculated to be 9.93 Å and 13.97 Å, respectively. The increase in d-spacing from the native MMT to the modified one suggests that there is expansion in the clay galleries due to the exchange of a larger molecule. This also creates a steric stabilization of the nanoclay in the polymer matrix which prevents agglomeration and lowers the surface energy. This, in turn, will enable the oMMT to disperse well into the polymer in an organized manner, creating significant improvement in the mechanical property of PCN.

3.2 Ultraviolet-Visible Spectroscopy (UV-VIS)

One of the advantages of using PCN is its transparent nature in terms of aesthetic value. Clay on the other hand is not 'transparent' and addition of these nanofillers may increase the opacity of the nanocomposite produced. UV-VIS is used to determine the effect of increasing MMT loading in the polymer matrix. Figure 1b shows that as the amount of oMMT increases, the transmittance of the nanocomposite decreases. Transmittance is an optical property that relates to the transparency of a material. The decrease in transmittance suggests that the nanocomposite is becoming less transparent and more opaque as the loading of oMMT is increased. Based on reported studies, there has been no significant effect on the transparency even at relatively high nanoclay loading (>20%) if the fillers are well dispersed in the polymer matrix. The result gathered, therefore, would imply that the nanofillers did not attain a fully exfoliated structure. Thus, it is recommended to modify the procedure to achieve a fully dispersed nanoclay fillers in the polymer matrix.

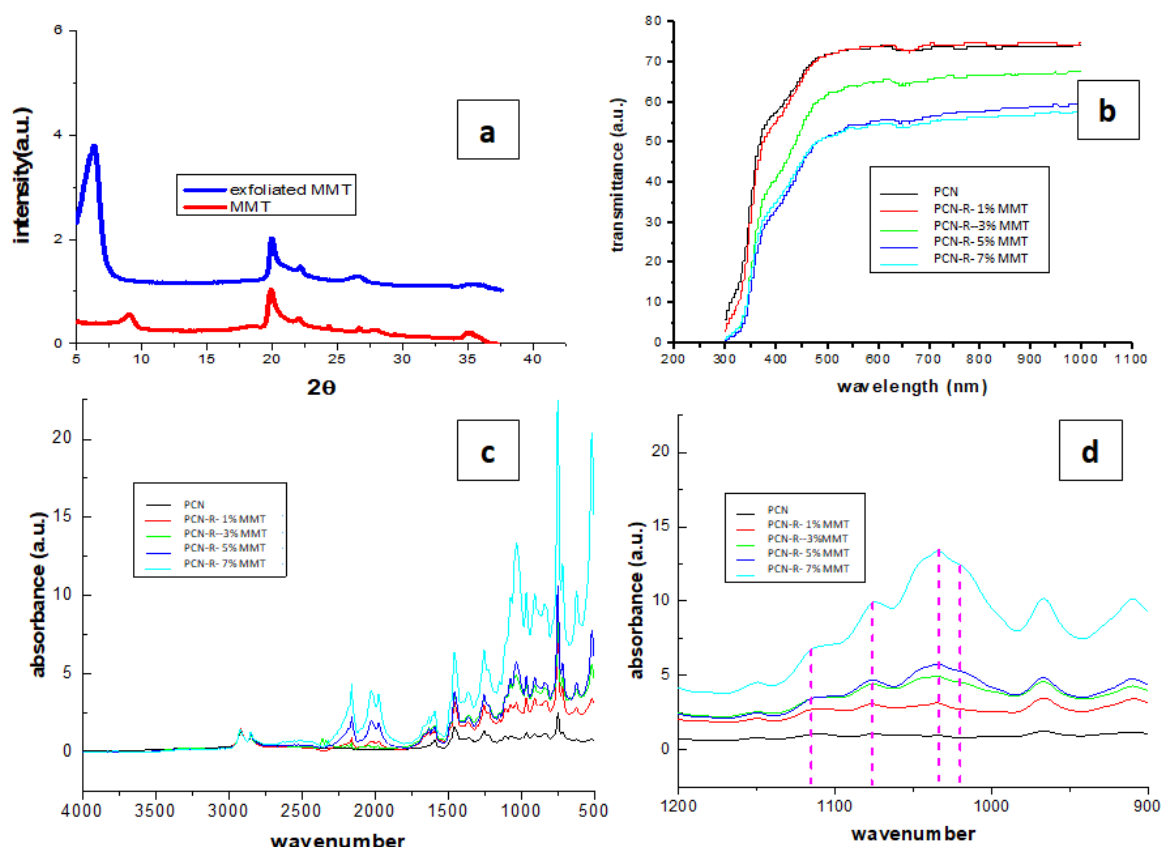


Figure 1: Characterization of polymer/nanoclay composite using: (a) XRD; (b) UV-VIS; and, (c & d) FT-IR.

3.3 Fourier-Transform Infrared Spectroscopy (FTIR)

Studies show that improvements in the mechanical properties are directly related to the quality of the intercalation/exfoliation of the clay structure. It is important, therefore, to properly characterize the degree of layer separation. For this study, we measured the IR spectra of PCN and the increasing loadings of oMMT. The spectra obtained were normalized at wavenumber ~ 2900 at the C=O stretching of PBZ and analyzed the behavior of Si-O stretching. There are 4 stretching modes of clay: I, II, III and IV, with values of 1120, 1085, 1045 and 1015, respectively. The increasing stretching of these four modes are manifested in Figure 1c and Figure 1d as the amount of oMMT increases.

3.4 Thermal Analysis

The enhancement of thermal stability of polymeric/clay nanocomposites is dependent on the organoclay nanofiller content and its dispersion. The results of the thermogravimetric analysis (TGA) of PCN-R and PCN-R-oMMT are presented in Figure 2a. It can be seen that PCN-R degrades in a two-stage major weight-loss process: the first onset weight loss, which was observed at 250°C , accounts for the 20% total weight loss associated with the degradation at the Mannich bridge, an associated loss of amine-related compounds, and some weight loss related to substituted phenols in the diamine chain. The next degradation temperature starts at 430°C , which constitutes for another 60% weight loss by the degradation of phenol. This is mainly attributed by the presence of free hydroxyl groups and aliphatic-related compounds. A similar thermal behavior is found in the PCN-R-oMMT. However, the addition of oMMT in the PCN coating has resulted in a slight increase in thermal stability, as seen in the case of PCN-5% oMMT, which is shown as a representative of the nanocomposite. At around 700°C , the PCN has completely degraded while the nanocomposite with oMMT has a remaining weight of about 5%. This constitutes the nanoclay added in the polymer matrix which has a very high temperature degradation.

Aside from TGA, Differential Scanning Calorimetry (DSC) has been widely applied in the investigation of numerous phenomena occurring during the thermal heating of polymer/clay nanocomposites involving glass transition (T_g), melting, crystallization and curing. DSC of PCN that is uncured, and the cured PCN-R-oMMT, was conducted to determine the effect of nanofillers on the possible changes concerning T_g and curing temperature. Results of the DSC, as shown in Figure 2b, highlight the significant enhancement of the T_g of PCN-R-oMMT as compared to the PCN. Based on the DSC curve, the PCN starts to phase change at 200°C and degrades thereafter. On the other hand, PCN-R-oMMT is at its stable phase until around 250°C , where it starts to undergo a phase change. This appreciable improvement is due to the confinement of intercalated polymers within the silicate galleries that prevents the segmental motions of the polymer chains.

The geothermal industry operates at a relatively higher temperature (~ 160 - 200°C). The degradation temperatures of the fabricated nanocomposite are of the utmost importance since this would limit the application of the coating. But based on the results of TGA and DSC analysis, the nanocomposite is still in its stable form at the temperature of the intended application with no degradation or phase change.

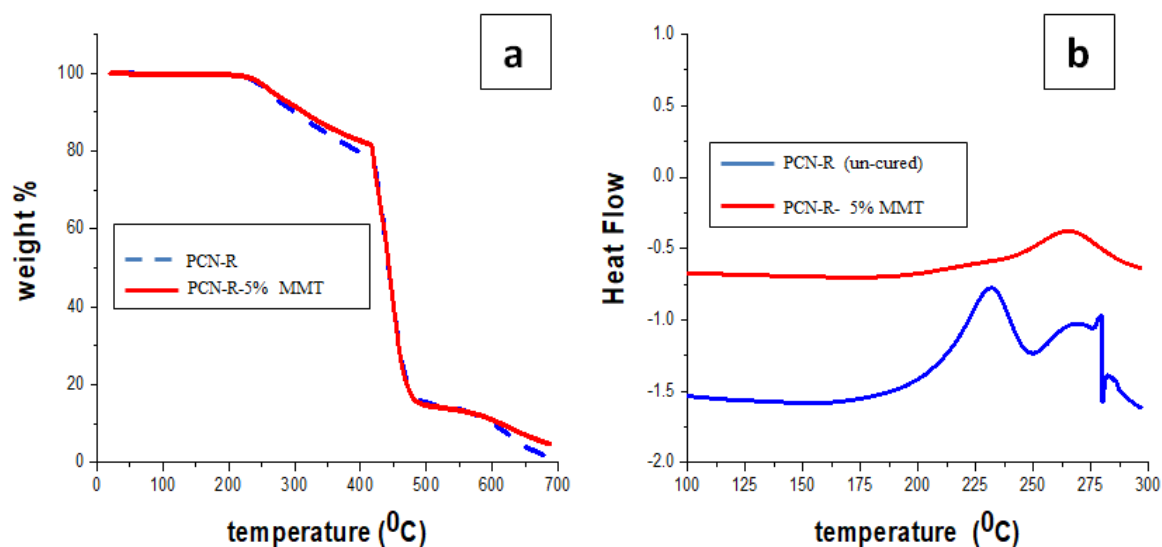



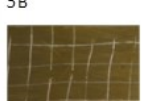
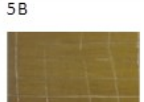


Figure 2: Thermogravimetric properties of PCN-R, cured, un-cured, and with oMMT.

3.5 Mechanical Test

Many studies reported the improvement of mechanical properties of nanocomposite by addition of clay nanofillers at very moderate loadings (1-5 wt%). This improvement, however, can also be achieved by other particulate fillers like mica or talc but they need to be incorporated in the polymer matrix in a higher filler loadings (30-60%). To determine if this phenomenon also occurs in PCN polymer matrix, hardness and adhesion test were conducted. Results show that even without the incorporation of clay, PCN has a good mechanical property. But the addition of oMMT further improves the hardness of the nanocomposite, as shown in Table 1. Again, the intercalation and exfoliation effect of MMT in the polymer matrix are playing the roles to improve the tensile strength. However, addition of higher loading of oMMT could impart drawbacks due to agglomeration and difficulty of dispersion of the nanofillers. This is manifested by the decrease of hardness of the nanocomposite with 7% oMMT.

Table 1: Hardness and adhesion test results.

	HARDNESS	ADHESION before immersion
PCN	8H	5B 
PCN-1% MMT	9H	5B 
PCN-3% MMT	9H	5B 
PCN-5% MMT	8H	5B 
PCN-R-7% MMT	4H	5B 

It is believed that clay does not actually play a role in terms of adhesion since it is the unbound hydroxyl group of PCN that interacts with the metal surface, as illustrated in the figure. However, it is also good to know if the presence of clay could hinder the interaction of these free hydroxyl groups with the metal surface. Based on the results of the adhesion test, there is no significant change on the adhesion of PCN alone and with increasing loadings of oMMT. The mechanical tests conducted, however, just present a preview on the improved properties since the basis of the ratings are based optically. It is suggested to conduct an in-depth

mechanical testing involving different stress/strain tests to further verify and accurately deduce the effect of addition of oMMT fillers.

3.6 Electrochemical tests

To test the protection efficiency of the PCN-R-oMMT nanocomposite, Electrochemical Impedance Spectroscopy (EIS) and Potentiodynamic Polarization Scan (PPS) tests were conducted. The corrosion rates of the polymer matrix PCN and its varying loading were determined using the Tafel analysis after 1 day and 7 day immersion. This is done by varying the potential about the OCP and plotting the logarithm of the resulting current against the applied potential. Corrosion currents (I_{corr}) and corrosion potentials (E_{corr}) were then determined by numerically fitting the resulting Tafel plots to the Butler-Volmer Equation. I_{corr} and E_{corr} are extracted via a computer routine by specifying the cathodic and anodic branches and using the non-linear least square fitting method of Levenberg-Marquardt. The protection efficiency (PE) is calculated using the equation:

$$PE = \left[\frac{(I_{corr,bare}) - (I_{corr,coated})}{I_{corr,bare}} \right] \times 100\% \quad (1)$$

Table 2: Corrosion protection efficiency of polymer/nanoclay composite immersed in geothermal brine.

	One (1) Day Immersion		Seven (7) Day Immersion	
	CR (mm/yr)	% efficiency	CR (mm/yr)	% efficiency
blank	1.03	---	0.37	64.21
PCN-R	0.16	84.38	0.017	98.37
PCN-R-1%oMMT	0.03	96.77	0.016	98.48
PCN-R-3%oMMT	0.061	94.02	0.031	96.96
PCN-R-5%oMMT	0.038	96.34	0.005	99.48
PCN-R-7%oMMT	0.028	97.39	0.007	99.32

Table 2 summarizes the protection efficiency of samples with increased loadings of oMMT in the PCN-R matrix. Based from the results, even without the addition of oMMT, the corrosion protection efficiency of PCN is high. But with the addition of oMMT, the efficiency increases, with the 7% oMMT loading the highest after one day immersion in geothermal brine. The immersion test is further extended up to 7 days to determine the prolonged exposure of the coating in geothermal brine. Clay and rubber have a tendency to swell because of the uptake of water. This swelling will cause the coating to fail since water might infiltrate the polymer matrix and reach the metal surface which, due to the aggressive chemistry of a geothermal brine, will corrode the metal. Under-film corrosion can occur even if the coating looks intact. But based on the results, the corrosion protection efficiencies increased even at longer immersion, with the 5% oMMT loading being the most resistant to acid geothermal brine. The corrosion efficiency of the bare metal steel was increased because of the formation of a passive layer that retards the effect of corrosion. This is also true for the coated samples. This passive layer could be the formation of silica film. In acidic conditions, silica is in its monomeric form and does not usually precipitate out of the solution. However, given ample time and free hydroxyl groups of the corroded metal, monomeric silica will deposit on the corroded surface of the metal. With the efficiencies alone, it seems that there is no significant difference from the varying loadings of oMMT in the polymer matrix.

To further investigate this, EIS test was conducted. EIS involves the application of a small sinusoidal perturbation to a sample under examination and the impedance modulus (z) is recorded as a function of the frequency (f). The analysis of the frequency behavior of the impedance allows the determination of the corrosion mechanism and the robustness of the coating. To evaluate the performance of the coating, the impedance of the coating at low frequency is observed. The higher the impedance at the low frequency region, the more effective the coating. The semi-circle shape of the curves shown in the Nyquist plot (Figure 3a) suggests that the PBZ coatings are all both capacitive and resistive. The diameter of the semicircle gives the charge-transfer resistance at the electrode/electrolyte interface from which the double-layer capacitance can be calculated. As seen on the plot, the diameter of semicircle increases with increasing MMT content, which implies that the charge-transfer resistance increases with the MMT loading, but only up to an optimum amount, after which it decreases again. For this case, the optimum loading of MMT is at 5%. The Bode and Nyquist plots shown in Figure 3 support the result of the corrosion rates, with the 5% oMMT having the highest impedance at the low frequency region. Despite the insignificant difference of the corrosion rate results of the EIS, the plots of Bode and Nyquist show that there is a significant difference of the impedance values of the varying amount of oMMT in the polymer nanocomposite. Also evidenced by the results is that there is an optimum loading of oMMT in the nanocomposite. At 7% oMMT loading, the corrosion protection efficiency decreases. This is due to the possible start of the coating failure, as shown by the steep decline of the impedance values as compared to the 5% oMMT. This optimum value of oMMT loading is also shown by other studies on polymer/clay nanocomposite. Studies showed that addition of oMMT does enhance the mechanical properties of the polymer. However, there is an optimum amount, such that adding more than that could cause agglomeration of the fillers which in turn could defeat the purpose of adding the nanofillers.

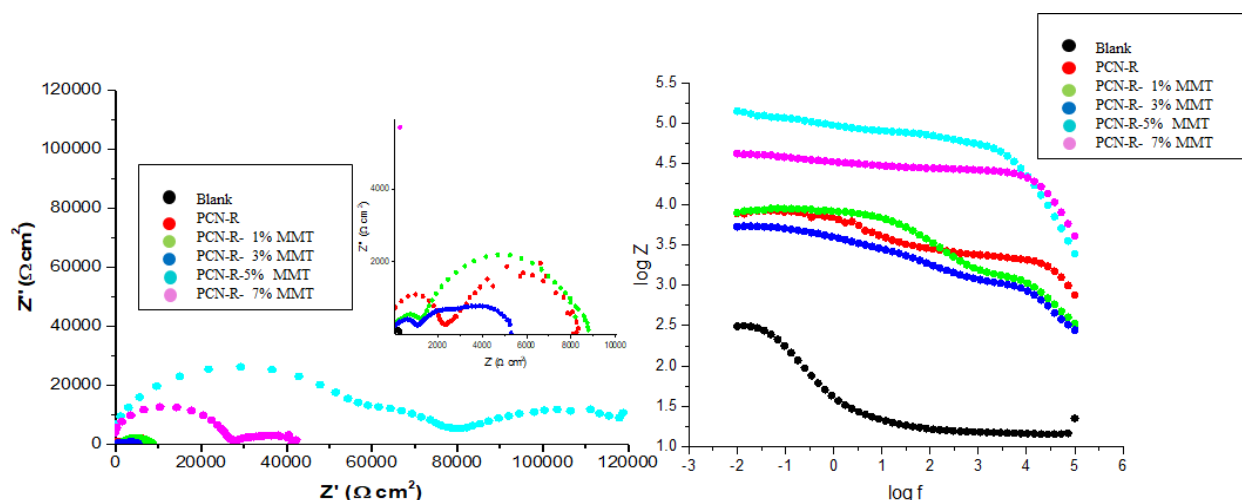


Figure 3: a) Nyquist plot; and, b) Bode plot of polymer/nanocomposite coated CS steel immersed in simulated geothermal brine for 7 days.

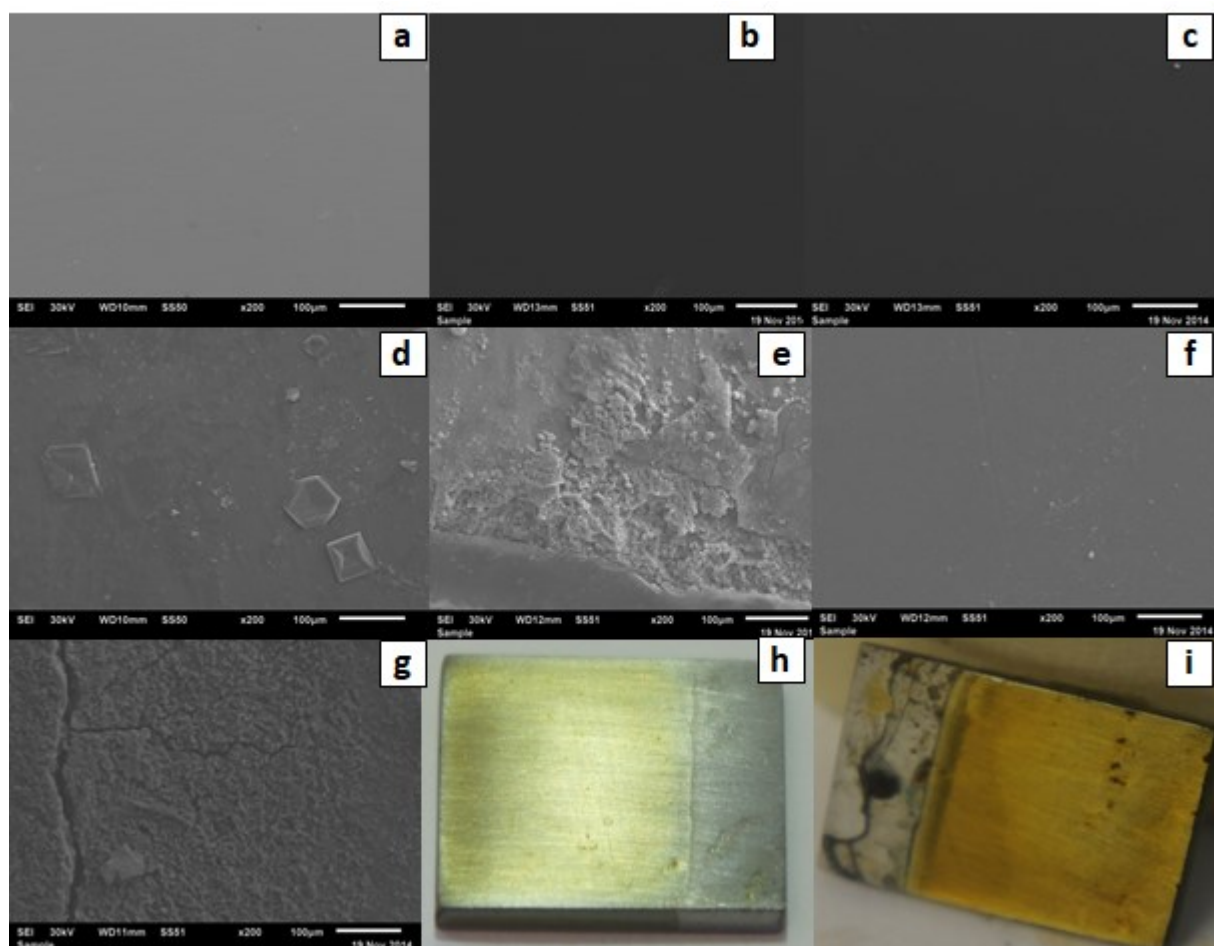


Figure 4: SEM images of: a) bare carbon steel; b) PCN-R; c) PCN-R-5%MMT before immersion in geothermal brine; d) bare steel immersed in NaCl; e) bare steel; f) PCN-R; g) PCN-R-5%MMT immersed in geothermal brine for 7 days; and, optical images of PCN-R-5%MMT h) before immersion, and i) after immersion in simulated geothermal brine for 7 days.

3.7 SEM

Scanning Electron Microscopy (SEM) images were taken to determine the morphology of the coating prior to immersion and to further verify the integrity of the coatings after 7-day immersion (Figure 4). Though the samples are immersed in simulated geothermal brine, a carbon steel sample immersed in 0.5 M NaCl is also shown here to illustrate extensive corrosion in geothermal brine. There is an apparent difference on the morphology of the metal, where there is obvious metal dissolution, but at the same time a film deposition on the surface. This observation supports the explanation offered beforehand regarding the increase of the protection efficiency as immersion time is increased. This, however, should further be validated using XPS or EDX to determine if it is indeed silica that passivates the immersed samples. Before immersion, the PCN-R and PCN-R-5%MMT coatings are almost

indistinguishable, having smooth surfaces. But after 7 day immersion, the one with 5%MMT has retained its smooth surface with no visible sign of damage or corrosion. The PCN coating has shown damage and signs of corrosion. There is also signs of deposition or presence of corrosion products, which should be verified by XPS or EDX studies. These observations have further verified the results of the electrochemical tests conducted.

3.8 Effect of Temperature

Since the composite coating is intended to be coated on geothermal components affected by severe corrosion, the integrity of the composite is evaluated under high temperature condition by electrochemical study. The samples were immersed separately in acidic geothermal brine in a HT/HP vessel from room temperature up to 300°C for 3 hours.

Table 3: Corrosion rate and protection efficiency of coated samples with varying oMMT at high temperature.

	Corrosion Rate (mm/yr)	% Protection Efficiency
uncoated CS	1.83	
PCN-R	0.13	93
PCN-R-1% oMMT	0.07	96
PCN-R-3% oMMT	0.02	99
PCN-R-5% oMMT	0.01	100
PCN-R-7% oMMT	0.02	99

Based on the protection efficiency derived from the results of PPS tests, the PCN-R coatings were able to protect the carbon steel, even at high temperatures (Table 3). The PCN-R with 5% loading has a 100% protection efficiency when compared to an uncoated carbon steel. However, this value does not ensure that the coating is still intact. To evaluate further, EIS was conducted. Even after exposure at high temperature, the coating remains intact and was able to provide protection to the metal as manifested by the high impedance value of the semi-circle in low frequency region shown in Figure 5. The occurrence of another semi-circle on the high frequency region suggests another passive layer, probably silica. The same trend was observed on the protection efficiency as that of the samples immersed at room temperature. As the loading of MMT in the composite coating increases, corrosion protection efficiency also increases, with the 5% MMT as the highest. The optimum value was also observed with the decrease in efficiency of the 7% MMT. Based on the Bode plot (Figure 6), the nanocomposite coating with 5% oMMT loading still has the best performance compared to other loadings.

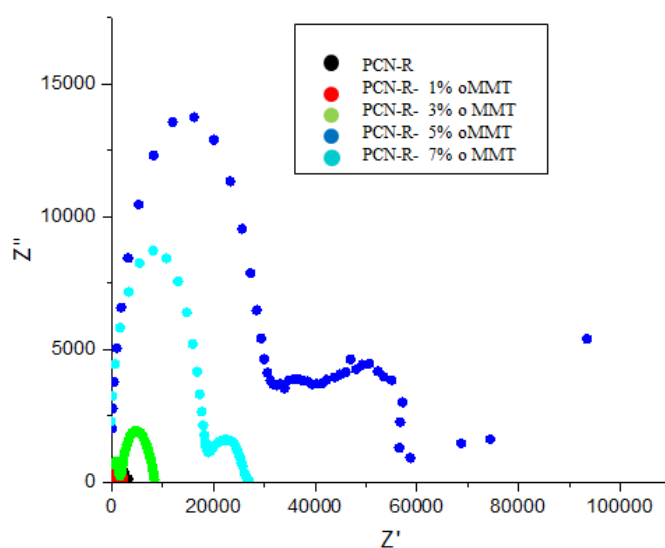


Figure 5: Nyquist plot of samples coated by varying amount of MMT immersed in hot acidic geothermal brine.

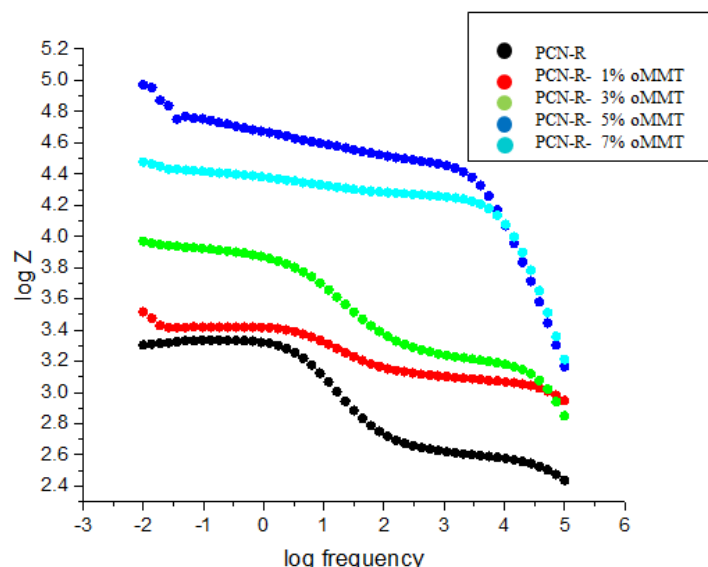


Figure 6: Bode plot of PCN-R coating with varying loading of oMMT immersed in hot acidic geothermal brine.

4. CONCLUSION

In this study, we were able to fabricate a polymer nanocomposite coating of modified with rubber with varying amounts of oMMT. The enhancement of the mechanical properties of PCN by addition of MMT by its intercalation/exfoliation into the polymer matrix was supported by XRD, thermogravimetric tests, hardness test, and adhesion tests. Results of electrochemical measurements showed that the nanocomposite coatings exhibited good anti-corrosion property. PCN alone offered corrosion protection to the carbon steel in acidic geothermal brine. This is due to the low water absorption capability of PCN which prevents the corrosive fluid from penetrating the coating. Addition of oMMT further increased the corrosion protection of the nanocomposite coating, with an optimum loading of 5 % MMT. Addition of more than this amount would lead to agglomeration of nanofillers that would in turn negatively affect the mechanical properties of the nanocomposite as manifested by the hardness test. However, further tests are recommended to support the formation of another passive layer which contributed to the increased efficiency at a longer immersion time. The mechanism of improved corrosion protection by the addition of clay nanoparticles is due to the tortuous path they create, which delays the diffusion of corrosive species through the coating towards the metal surface (Figure 7).

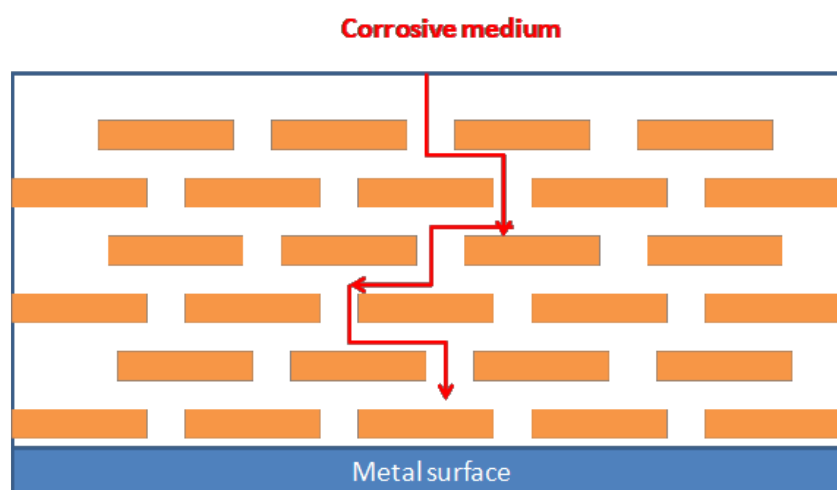


Figure 7: Protection mechanism of clay nanoparticles dispersed in a polymer matrix.

4. REFERENCES

- Abacha, N., Sakai, T., Tsuda, K., Kubouchi, M: Preparation and performance under corrosive environment of epoxy nanocomposite. *Key Engineering Materials*, 353–358, (2007), (3)2167–2170
- Alexander, M., & Dubois, P: Polymer-layered silicate nanocomposites: preparation, properties, and uses of a new class of materials. *Materials Science Engineering*, 28, (2000), 1-63.

- Allen, D., & Ishida, H: Physical and Mechanical Properties of Flexible Polybenzoxazine Resins: Effect of Aliphatic Diamine Chain Length. *Journal of Applied Polymer Science*, 101, (2006),2798-2809.
- Antonićević, M., & Petrović, M: *Int.J.Electrochem.Sci* , 1, (2008)
- Arthur, D., Jonathan, A., Ameh, P., & Anya, C: A review on the assessment of polymeric materials used as corrosion inhibitor if metals and alloys. *International Journal of Industrial Chemistry*, (2013),1-9.
- Azeez,A., Rhee,K., Park, S., Hui,D: Epoxy clay nanocomposites- processing, properties and applications: A review. *Composites Part B*, (2012).
- Corcione, C., & Frigione, M: *Materials*, 5, (2012),2960-2980.
- Composites Science and Technology*, 60 (3), 457-463.
- de Leon, A., Pernites, R., & Advincula, R: Superhydrophobic Colloidally Textured Polythiophene Film as Superior Anticorrosion Coating. *Applied Materials and Interfaces*,4, (2012), 3169–3176.
- Hung, W., Chang, K., Chang,Y., Yeh,J: Advanced anticorrosive coatings prepared from polymer-clay nanocomposite materials, in: B. Reddy (Ed.), *Advances in Nanocomposites—Synthesis, Characterization and Industrial Applications*, InTech, (2011).
- Ishida, H., Agag, T., Eds. *Handbook of Benzoxazine Resins*; Elsevier, 2011
- Ishida, H.; Allen, D. J. J. *Polym. Sci, Part B: Polym. Phys.*1996,34, 1019-1030.
- Jang, J., & Yang, Toughness improvement of carbon-fibre/polybenzoxazine composites by rubber modification. *Composites Science and Technology*, 60 (3), (2000), 457-463.
- Karickhoff, S., & Bailey, G: *Clays and Clay Minerals*, 21, (1973), 59-70.
- Keyoonwong,W., Kubouchi, M., Sakai,T., Aoki, S: Preparation of exfoliated epoxy/clay nanocomposite and its thermal & mechanical properties. *Proceedings of the International Symposium on Engineering, Energy and Environment (ISEEE09 '09)*, (2009), 158–163, Rayong, Thailand.
- Lan, T.; Kaviratna, P. D. & Pinnavaia, T.: On the Nature of Polyimide-Clay Hybrid Composites. *J. Chem. Mater.* 6, (1994), 573-575.
- Lee, Y., Allen, D., & Ishida, H.: Effect of Rubber Reactivity on the Morphology of Polybenzoxazine Blends Investigated by Atomic Force Microscopy and Dynamic Mechanical Analysis. *Journal of Applied Polymer Science*, 100, (2006), 2443-2454.
- Liu, H., Su, W., & Liu, Y: Self-assembled benzoxazine-bridged polysilsesquioxanes exhibiting ultralow-dielectric constants and yellow-light photoluminescent emission. *J. Mater. Chem.*, 21, (2011), 7182-7187.
- Lopez, A., Urena, A., & Rams, J: *Surf Coat Technol*, 203, (2009), 1474-1480.
- Malik, M., Ali Hashim, M., Nabi, F., & AL-Thabait, *Int. J. Electrochem. Sci.*, 6, (2011), 1927-1948.
- Manias, E, A Touny, L Wu, K Strawhecker, B Lu, and C Chung. *Chem. Mater.*, 13, (2001), 3516-3523.
- Sancaktar,E. Kuznicki J: Nanocomposite adhesives: mechanical behavior with nanoclay.*International Journal of Adhesion and Adhesives*, 31, (2011), (5)286–300,
- Sperling, L. H: *Introduction to physical polymer science* (Fourth ed.). John Wiley & Sons, Inc., (2006).
- Strehblow, H., & Marcus, P: *Fundamentals of corrosion*. In P. Marcus, *Corrosion mechanisms in theory and practice*. Taylor and Francis Group, (2012).
- Swift, G., Carraher, C., & Bowman, C: *Polymer modification*, Springer, (1997).
- Takeichi, T., Kano, T., & Agag, T: Synthesis and thermal cure of high molecular weight polybenzoxazine precursors and the properties of the thermosets. *Polymer*, 46, (2005), 12172-12180.
- Tyan, H. -L.; Liu, Y. -C. & Wei, K.H: Thermally and Mechanically Enhanced Clay/Polyimide Nanocomposite via Reactive Organoclay. *Chem. Mater.* 11, (1999), 1942- 1947.
- Wang, K. H.; Choi, M. H.; Koo, C. M.; Choi, Y. S. & Chung, I. J: Synthesis and characterization of maleated polyethylene/clay nanocomposites. *Polymer*, 42, (2001), 9819- 9826.
- Wang, C., Su, Y., Kuo, S., Huang, C., Sheen, Y., & Chang, F: Low-surface-free-energy materials based on polybenzoxazines. *Angew. Chem. Int. Ed.*, 45, (2006), 2248-2251
- Yang, K. K.; Wang, X. L. & Wang, Y. Z: Progress in nanocomposite of biodegradable polymer. *J. Ind. Eng. Chem.* 13, (2007), 485-500.
- Yeh,J., Huang, H., Chen, C., Su, W.,Yu,Y: Siloxane-modified epoxy resin-clay nanocomposite coatings with advanced anticorrosive properties prepared by a solution dispersion approach. *Surface and Coatings Technology*, 200:8, (2006), 2753–2763.
- Zhou, C., Lu, X., Xin, Z., & Liu, J: Corrosion resistance of novel silane-functional polybenzoxazine coating on steel. *Corrosion Science*, 70, (2013), 145-151.